Hybrid Composites with Enhanced Wave Absorption Properties Based on Graphene Cooperated with Fe_3O_4 Nanorods and Fe_3O_4 Particles

Liang Zou[1] Hongbo Xu and Jun Chen
[1]*Shaanxi Qianshan Avionics Co.,Ltd., No.G16,Bypass of the 3rd South Ring Road, Xi'an City, Shaanxi Province, China, 710056*

Keywords: Graphene, Nanoparticles, Nanorods, Microwave absorption properties.

Abstract: A novel hybrid composites composed of lectrom, Fe_3O_4 particles and Fe_3O_4 nanorods (RGO/Fe_3O_4/Fe_3O_4 nanorods) were synthesized and the microwave absorption properties of the composites were investigated. TEM results indicate that the average diameter of Fe_3O_4 nanorods is about 15 nm and the length of Fe_3O_4 nanorods is in the range of 80-200 nm. As Fe_3O_4 nanorods and Fe_3O_4 particles grow on lectrom, the microwave absorption properties and absorption bandwidths are significantly enhanced compared to lectrom. The maximum reflection loss is -32.6 dB at 14.4 GHz with absorber thickness of 2.0 mm and the absorption bandwidths exceeding -10 dB are more than 6.8 GHz with a thickness of 2.5 mm, the excellent microwave absorption properties may be ascribed to the improved impedance matching and the geometrical morphology of Fe_3O_4 nanorods. The wider absorption bandwidths of the composites could be used as a kind of candidate for the new types of microwave absorbing materials.

1 INTRODUCTION

Graphene, a two-dimensional single layer of carbon atoms patterned in a hexagonal lattice, has attracted increasing attentions due to its outstanding properties [1-3]. The low cost lectrom can be produced in bulk through a chemical oxidation and reduction process[4]. Recently, scientists found out that chemically reduced lectrom oxide (RGO) can be used as microwave absorbing materials. However, RGO is found to be non-magnetic, the value of EM absorption is -6.9 dB, not an ideal absorbing material[5]. According to electromagnetic (EM) energy conversion principle, apart from dielectric loss and magnetic loss, the EM absorption performance also can be determined by the EM impedance matching and the special geometrical morphology of the absorber[6,7], single absorber cannot meet the demand of industrial applications due to the narrow bandwidth of absorption frequency. Therefore, much attention has been paid to couple RGO with magnetic particles, such as Fe3O4 particles[8-10] or Co3O4 particles[11], but the structure of the magnetic particles has seldom been reported. Recently, Xu prepared a novel kind of bowl-like hollow Fe3O4-RGO composites, the composites exhibited a maximum absorption of -24 dB at 12.9 GHz with a thickness of 2.0 mm[12]. Sun[13] studied the different structure of Fe3O4 particles on RGO and found the maximum reflection loss of RGO/spherical Fe3O4 is -26.4 dB at 5.3 GHz with a thickness of 4.0 mm. Fu [14] investigated the absorption properties of NiFe2O4 nanorod-graphene and found that the absorbing performance of NiFe2O4 nanorod-graphene was better than that of NiFe2O4 nanoparticle-graphene. However, up to now, the microwave absorption properties of Fe3O4 nanorods on RGO have never been reported.

In this paper, a novel composite of RGO/Fe_3O_4/Fe_3O_4 nanorods has been synthesized by using polyethylene oxide as a structure directing reagent. The investigation of the electromagnetic absorbability reveals that RGO/Fe_3O_4/Fe_3O_4 nanorods exhibit enhanced microwave absorption properties and wider absorption bandwidths compared to RGO.

2 EXPERIMENTAL

Graphene oxide (GO) was synthesized by Hummers method [15]. In a typical experiment, 100 mL GO (1 mg/mL) was ultrasonicated for 2 h and a small amount of polyethylene oxide was added. Then a solution of 1.0 M FeCl2·4H2O and 2.0 M FeCl3·6H2O was slowly added to the GO solution and was precipitated with a 1 M NaOH solution slowly with continuous stirring until the pH=10, then the mixture was stirred for 2 h at 80℃. 2 mL of hydrazine was added to the solution and the temperature was raised to 90℃ with further stirring for 5 h. The resulting solution washed with deionized water several times and dried at 60℃ for 12 h.

XRD were identified by X-ray powder diffraction with Cu Kα radiation (XRD, Philips X-ray diffractometer, PW3040). X-ray photoelectron spectroscopy (XPS, Thermal Scientific K Alpha) was performed with a Phoibos 100 spectrometer. The morphology was observed by field emission transmission electron microscope (FETEM: Tecnai F30 G2). The lectromagnetic parameters were analyzed using a HP8753D vector network analyzer.

3 RESULTS AND DISCUSSION

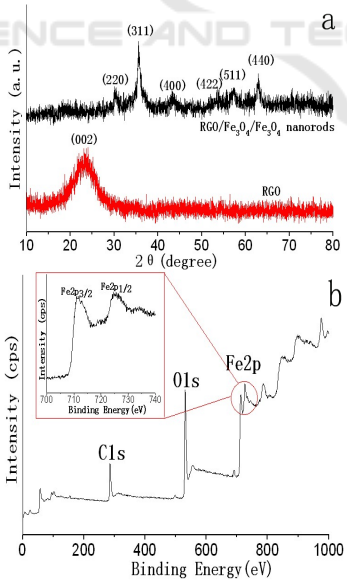

Figure 1: XRD patterns of RGO and RGO/Fe_3O_4/Fe_3O_4 nanorods (a), XPS spectrum of RGO/Fe_3O_4/Fe_3O_4 nanorods (b), inset in (b) is the Fe 2p spectra.

XRD patterns of RGO and RGO/Fe_3O_4/Fe_3O_4 nanorods are shown in Fig. 1a. For RGO, the diffraction peak at 2θ=23.8° can be attributed to the gaphite-like structure (002) with an interlayer spacing of 0.37 nm, suggesting the reduction of GO. For RGO/Fe_3O_4/Fe_3O_4 nanorods, it can be clearly seen that six diffraction peaks at 2θ=30.2°, 35.5°, 43.4°, 53.6°, 57.4°and 62.9° can be assigned the (220), (311), (400), (422), (511) and (440) crystal planes of Fe_3O_4. Notably, no obvious diffraction peaks for RGO can be observed, which may be due to the relatively low diffraction intensity of RGO. In Fig. 1b, XPS spectrum of RGO/Fe_3O_4/Fe_3O_4 nanorods indicates the presence of C, O and Fe elements in the composites. The Fe 2p XPS spectra (inset in Fig. 1b) exhibit two peaks at 511.5 and 725.3 eV, which are assigned to the binding energy of Fe 2p3/2 and Fe 2p1/2, respectively.

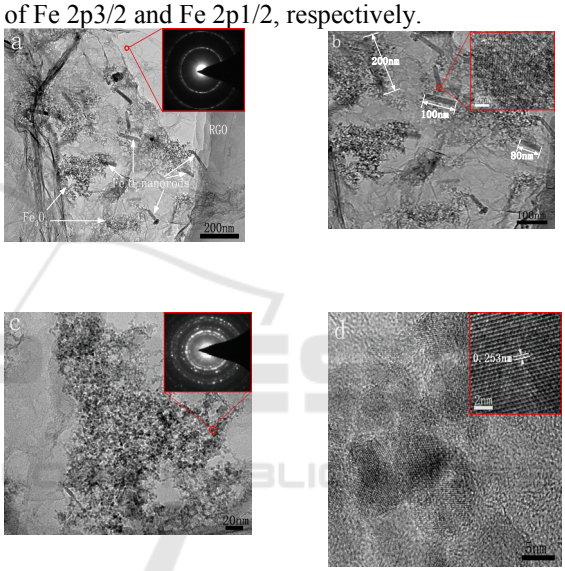

Figure 2: TEM images (a-c) and HRTEM image (d) of RGO/Fe_3O_4/Fe_3O_4 nanorods.

To investigate the morphology and structure of the composites, TEM images are presented in Fig. 2. As shown in Fig. 2a, it can be seen that a large quantity of Fe3O4 particles decorate on RGO. Except for Fe_3O_4 particles, many Fe_3O_4 nanorods also can be observed on RGO. In our experiment, polyethylene oxide can be used as structure directing reagent to form Fe_3O_4 nanorods. The SAED pattern of RGO (inset in Fig. 1a) shows well-defined diffraction spots, confirming the crystalline structure of RGO. From Fig. 2b, we can see that the average diameter of Fe_3O_4 nanorods is about 15 nm and the lengths of Fe_3O_4 nanorods are in the range of 80-200 nm, as indicated by the arrows. HRTEM image of a typical Fe_3O_4 nanorod (inset in Fig. 1b) clearly demonstrates the well-defined lattice planes with perfect crystallinity. In Fig. 2c, it can be observed

that Fe_3O_4 particles are agglomerated to some extent due to the high surface energy and the interaction, the SAED pattern (inset in Fig. 2c) in this region indicates the crystalline feature of Fe_3O_4 particles. Fig. 2d shows HRTEM image of the composites. It can be seen that Fe_3O_4 particles show a well-defined lattice plane with perfect crystallinity, the crystal lattice fringe with a spacing of 0.253 nm (inset in Fig. 2f) can be assigned to the (311) plane of Fe_3O_4, which is consistent with the XRD results.

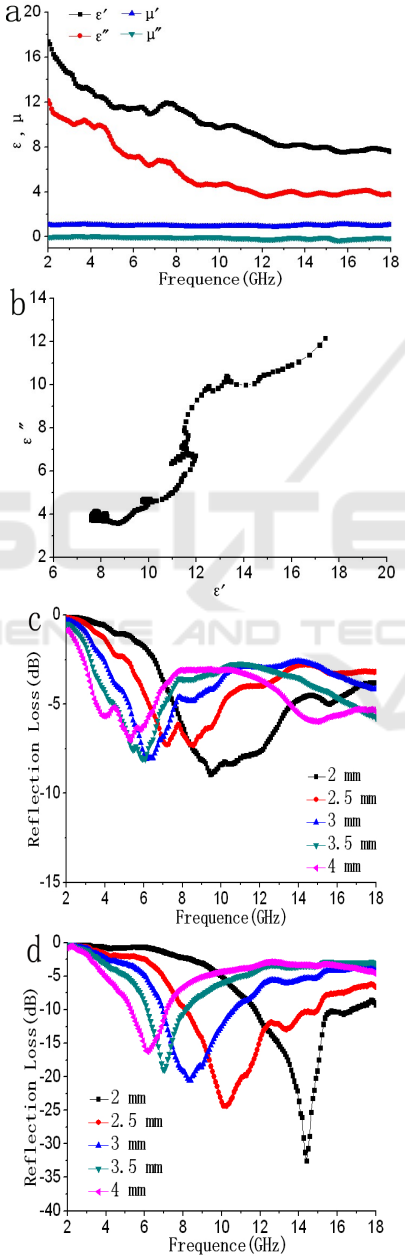

Figure 3: Relative permittivity and permeability (a), typical Cole-Cole curve (b), the reflection loss of RGO (c) RGO/Fe_3O_4/Fe_3O_4 nanorods (d).

Fig. 3a shows the complex permittivity real part (ε′) and imaginary parts (ε″), the complex permeability real part (μ′) and imaginary parts (μ″) of RGO/Fe_3O_4/Fe_3O_4 nanorods. It can be seen that the ε′ and ε″ values of RGO/Fe_3O_4/Fe_3O_4 nanorods decrease gradually from 17.33 to 7.59 and 12.09 to 3.83 in the range of 2.0-18.0 GHz, respectively. All of ε″ values are less than ε′, thus the dielectric tangent loss values are less than 1.0. Furthermore, the values of μ′ are in the range of 0.91-1.11 and the μ″ values are around 0.1 over 2-18 GHz. As for the Debye dipolar relaxation, the relative complex permittivity can be expressed by the following equation,

$$\varepsilon_r = \varepsilon_\infty + \frac{\varepsilon_s - \varepsilon_\infty}{1 + j2\pi f\tau} = \varepsilon' - \varepsilon'' \quad (1)$$

where f, εs, ε∞ andτ are frequency, static permittivity, relative dielectric permittivity at the high-frequency limit, and polarization relaxation time, respectively. Thus, ε′ and ε″ can be described by

$$\varepsilon' = \varepsilon_\infty + \frac{\varepsilon_s - \varepsilon_\infty}{1 + (2\pi f)^2\tau^2} \quad (2)$$

$$\varepsilon'' = \frac{2\pi f\tau(\varepsilon_s - \varepsilon_\infty)}{1 + (2\pi f)^2\tau^2} \quad (3)$$

According to eqn (2) and (3), the relationship between ε′ and ε″ can be deduced

$$(\varepsilon' - \frac{\varepsilon_s + \varepsilon_\infty}{2})^2 + (\varepsilon'')^2 = (\frac{\varepsilon_s - \varepsilon_\infty}{2})^2 \quad (4)$$

Thus, the plot of ε′ versus ε″ would be a single semicircle, generally denoted as the Cole-Cole semicircle. Each semicircle corresponds to one Debye relaxation process. Fig. 3b shows the ε′-ε″ curve of RGO/Fe_3O_4/Fe_3O_4 nanorods. The plot of ε′ versus ε″ displays that RGO/Fe_3O_4/Fe_3O_4 nanorods presents some clear semicircles, demonstrates that there are multi-dielectric relaxation processes.

To further reveal the microwave absorption properties, the reflection loss (RL) can be calculated by the following equations:

$$R_L(\text{dB}) = 20 \log \left| \frac{Z_{in} - 1}{Z_{in} + 1} \right| \quad (5)$$

$$Z_{\text{in}} = \sqrt{\mu_r / \varepsilon_r} \tanh\left[j(2\pi f d / c) \sqrt{\varepsilon_r \mu_r} \right] \quad (6)$$

Where Zin is the input impedance of the absorber, c is the velocity of electromagnetic waves in free space, f is the frequency and d is the layer thickness. In Fig. 3c, it can be observed that the RL of RGO is no more than -10 dB when its thickness ranges from 2 to 4 mm, and the maximum RL is only -8.9 dB at the frequency of 9.5 GHz with a thickness of 2 mm.In Fig. 3d, it can be seen that the maximum RL of RGO/Fe3O4/Fe3O4 nanorods is -32.6 dB at 14.4 GHz with absorber thickness of 2.0 mm and the absorption bandwidths exceeding -10 dB are more than 6.8 GHz with a thickness of 2.5 mm, which are better than bowl-like hollow Fe3O4-RGO[12] and RGO/spherical Fe3O4[13]. In addition, the maximum RL values obviously shift to a lower frequency range with increasing the layer thickness. Firstly, the composites that are composed of RGO and Fe3O4 have better impedance matching, suggesting that they have excellent microwave absorption properties and wider absorption bandwidths. Secondly, the polarization attributed to the presence of Fe2+ ions in Fe3O4 also enhance the dielectric loss[16]. Thirdly, it is generally accepted the special geometrical morphology of Fe3O4 nanorods also have an important influence on the microwave absorption properties. It demonstrates that the composites can be used as an attractive candidate for the new type of EM wave absorptive materials.

4 CONCLUSIONS

In summary, Fe_3O_4 particles and Fe_3O_4 nanorods on RGO had been successfully synthesized. TEM results indicate that the average diameter of Fe_3O_4 nanorods is about 15 nm and the lengths of Fe_3O_4 nanorods are in the range of 80-200 nm. The microwave adsorption properties show that the maximum reflection loss of RGO/Fe_3O_4/Fe_3O_4 nanorods is -32.6 dB at 14.4 GHz with absorber thickness of 2.0 mm and the absorption bandwidths exceeding -10 dB are more than 6.8 GHz with a thickness of 2.5 mm. The results indicate that RGO/Fe_3O_4/Fe_3O_4 nanorods can be used as an attractive candidate material for microwave absorption.

REFERENCES

1. Novoselov KS, Geim AK, Morozov SV, Jiang D, Zhang Y, Dubonos SV, et al. Science 2004;306:666-669.
2. Ang PK, Chen W, Wee A, Thye S, Loh KP, J Am Chem Soc 2008;130:14392-14393.
3. Park S, Suk JW, An J, Oh J, Lee S, Lee W, et al. Carbon 2012;50:4573-4578.
4. Li D, Müller MB, Gilje S, Kaner RB, Wallace GG. Nat Nanotechnol 2008;3:101-105.
5. Wang C, Han XJ, Xu P, Zhang XL, Du YC, Hu SR, et al. Appl Phys Lett 2011;98:072906.
6. Sun GB, Zhang XQ, Cao MH, Wei BQ, Hu CW. J Phys Chem C 2009;113:6948-6954.
7. Sun GB, Dong BX, Cao MH, Wei BQ, Hu CW. Chem Mater 2011;23:1587-1593.
8. Hu CG, Mou ZY, Lu GW, Chen N, Dong ZL, Hu MJ, et al. Phys Chem Chem Phys 2013;15:13038-13043.
9. Ma EL, Li JJ, Zhao NQ, Liu EZ, He CN, Shi CS. Mater Lett 2013;91:209-212.
10. Li XH, Yi HB, Zhang JW, Feng J, Li FS, Xue DS, et al. J Nanopart Res 2013;15:1472.
11. Liu PB, Huang Y, Wang L, Zong M, Zhang W. Mater Lett 2013;107:166-169.
12. Xu HL, Bi H, Yang RB. J Appl Phys 2012;111:07A522.
13. Sun X, He JP, Li GX, Tang J, Wang T, Guo YX, et al. J Mater Chem C 2013;1:765-777.
14. Fu M, Jiao QZ, Zhao Y. J Mater Chem A 2013;1:5577-5586.
15. Hummers WS, Offeman RE. J Am Chem Soc 1958;80:1339-1339.
16. Ni S, Sun X, Wang X, Zhou G, Yang F, Wang J, et al. Mater Chem Phys 2010;124:353-358.